Bulletin of the Geological Survey of Japan, vol. 71 (4), p. 313–330, 2020

Article

Late Jurassic radiolarians from mudstone near the U–Pb-dated sandstone of the North Kitakami Belt in the northeastern Shimokita Peninsula, Tohoku, Japan

UCHINO Takayuki[1,*] and SUZUKI Noritoshi[2]

UCHINO Takayuki and SUZUKI Noritoshi (2020) Late Jurassic radiolarians from mudstone near the U–Pb-dated sandstone of the North Kitakami Belt in the northeastern Shimokita Peninsula, Tohoku, Japan. *Bulletin of the Geological Survey of Japan*, vol. 71(4), p. 313–330, 7 figs, 1 table, 2 plates.

Abstract: In the northeastern Shimokita Peninsula, Aomori Prefecture, a Jurassic accretionary complex (AC) belonging to the North Kitakami Belt is distributed in three hilly areas of the Kuwabatayama, Katasakiyama and Omori. Although the AC in the Kuwabatayama area has been extensively studied and subdivided into the Late Jurassic Iwaya Unit and the Early Cretaceous Shitsukari Unit, those in the other areas are not fully understood except for a recent report of the detrital zircon U–Pb age from sandstone in the Omori area.

We extracted radiolarian fossils such as *Eucyrtidiellum* cf. *pyramis* indicating the Late Jurassic (probably Kimmeridgian) from mudstone near the U–Pb-dated sandstone in the Omori area. Because this radiolarian age is close to the zircon U–Pb age, and the horizons of the mudstone and sandstone are close without any recognizable distinctive tectonic discontinuity between them, the clastic rocks in the Omori area may be stratigraphically continuous or contemporaneous sequences deposited around the Kimmeridgian.

The ACs in the Katasakiyama and Omori areas are correlative to the Iwaya Unit in the Kuwabatayama area based on the lithology, geologic structure and clastic rock age. Therefore, the ACs in the northeastern Shimokita Peninsula can be divided into the Late Jurassic and the Early Cretaceous units; the former is the Iwaya Unit in the Kuwabatayama area and the unnamed ACs in the Omori and Katasakiyama areas, while the latter is the Shitsukari Unit in the Kuwabatayama area.

Keywords: radiolarian fossil, Late Jurassic, Kimmeridgian, accretionary complex, Shimokita Peninsula, North Kitakami Belt, Northeast Japan

1. Introduction

The North Kitakami Belt, located in the northern region of the Kitakami Massif of Tohoku (Northeast Japan), is mainly occupied by a Jurassic accretionary complex (AC). This AC is also sparsely exposed in the northward and westward areas of the massif because of the broad-scale coverage of Cenozoic volcanic and sedimentary rocks; only small amounts of the AC crop out in the Shimokita Peninsula, the south of Hirosaki City, the west of Lake Towada, the north of Mt. Hachimantai and the north of Mt. Moriyoshi (Fig. 1). A northeastern part in the Shimokita Peninsula, Aomori Prefecture, is marked by the Shimokita Hill, which is bounded by an escarpment along its east coast on the Pacific Ocean. The ACs in the northeastern Shimokita Peninsula are distributed in the Kuwabatayama, Katasakiyama and Omori areas from the north to south of Higashidori Village (Fig. 2a). The ACs in these areas are exposed as a coastal terrace with a 200- to 300-m elevated steep escarpment although they are mainly overlaid by the Neogene sediments of the Sunakomata or Tomari formations (Imai,1961) at the foot of the terrace. This paper mainly focuses on the ACs in the Katasakiyama and Omori areas.

The AC in the Kuwabatayama area crops out well along the seashore of Cape Shiriya and contains huge limestone blocks with fossils. Although it has been the subject of study by many researchers, the Katasakiyama and Omori areas have been little studied because of poor and fragmental exposures inland. Because the ACs in these two areas have not been mapped in detail despite the existence of 1:50,000 quadrangle series geologic maps, named “Chikagawa” (Imai, 1961) and “Shiriyazaki” (Tsushima and Takizawa, 1977), their geologic ages and

[1] AIST, Geological Survey of Japan, Research Institute of Geology and Geoinformation

[2] Department of Earth Science, Graduate School of Science, Tohoku University, Sendai 980-8578, Japan

[*] Corresponding author: UCHINO, T., Central 7, 1-1-1 Higashi, Tsukuba, Ibaraki 305-8567, Japan. Email: t-uchino@aist.go.jp

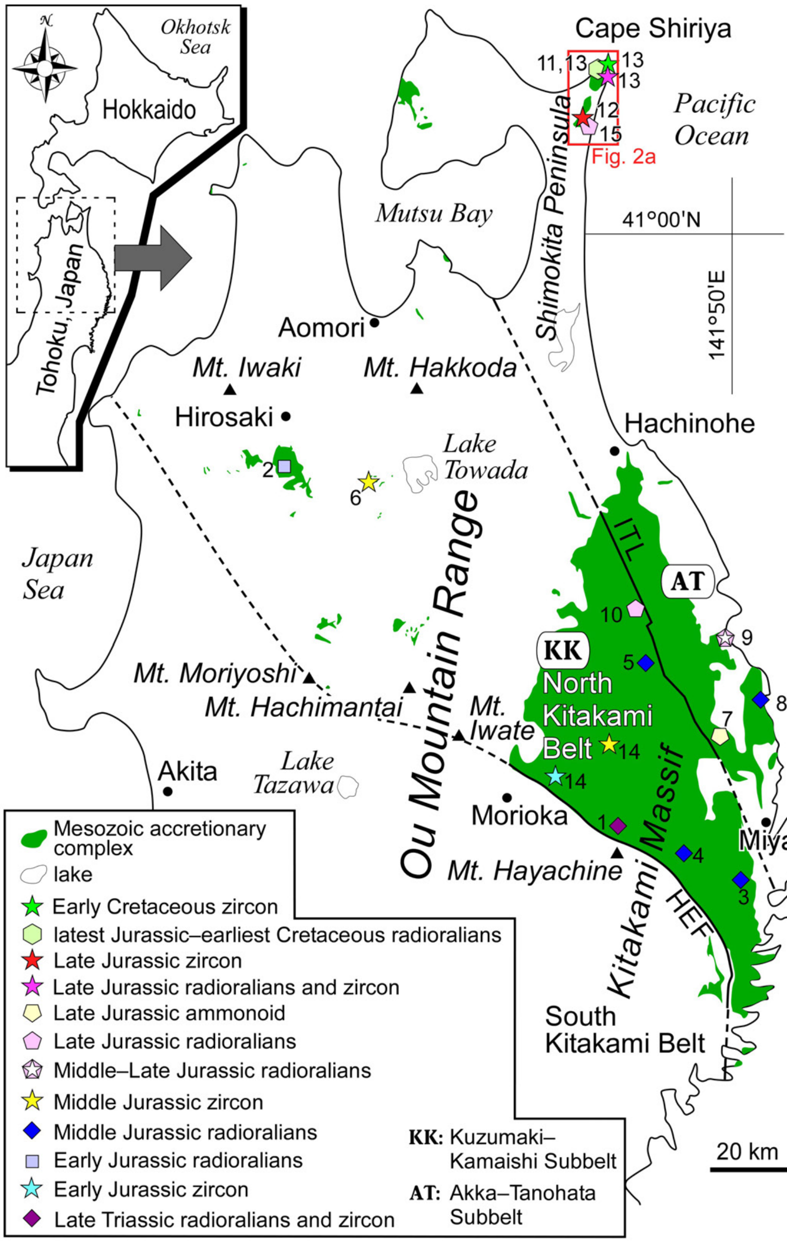

Fig. 1 Distribution map of Mesozoic accretionary complexes (green regions) in the North Kitakami Belt derived from the Seamless Digital Geological Map of Japan (1:200,000) V2 of the Geological Survey of Japan, AIST (2019). Symbols with numbers indicate the locations for which fossil and zircon ages from terrigenous clastic rocks were reported. 1: Kawamura *et al.* (2013); Uchino (2017), 2: Ueda *et al.* (2009), 3: Yoshihara *et al.* (2002); Suzuki and Ogane (2004), 4: Suzuki *et al.* (2007a), 5: Suzuki *et al.* (2007b); Ehiro *et al.* (2008), 6: Uchino (2018a), 7: Suzuki *et al.* (2007a), 8: Matsuoka and Oji (1990), 9: Minoura and Tsushima (1984), 10: Nakae and Kamada (2003), 11: Matsuoka (1987), 12: Uchino (2018b), 13: Ueda *et al.* (2018), 14: Uchino (2019), 15: this study.
HEF: Hayachine Eastern Marginal Fault, ITL: Iwaizumi Tectonic Line. The broken line shows an inferred fault.

tectonostratigraphy are not well understood. Recently, Uchino (2018b) obtained a zircon U–Pb age of ca. 155 Ma for the sandstone of the undated AC in the Omori area, indicating that it is slightly older than the latest Jurassic–earliest Cretaceous age for the clastic rocks (Matsuoka, 1987) in Cape Shiriya, which are regarded as the youngest in the North Kitakami Belt. To understand the tectonostratigraphy of the Shimokita Peninsula, more data, such as radiolarian fossil ages, are required for this region. This paper reports radiolarians from mudstone near the location of sandstone dated using detrital zircon U–Pb geochronology, and discusses the local geologic correlation based on lithology and ages.

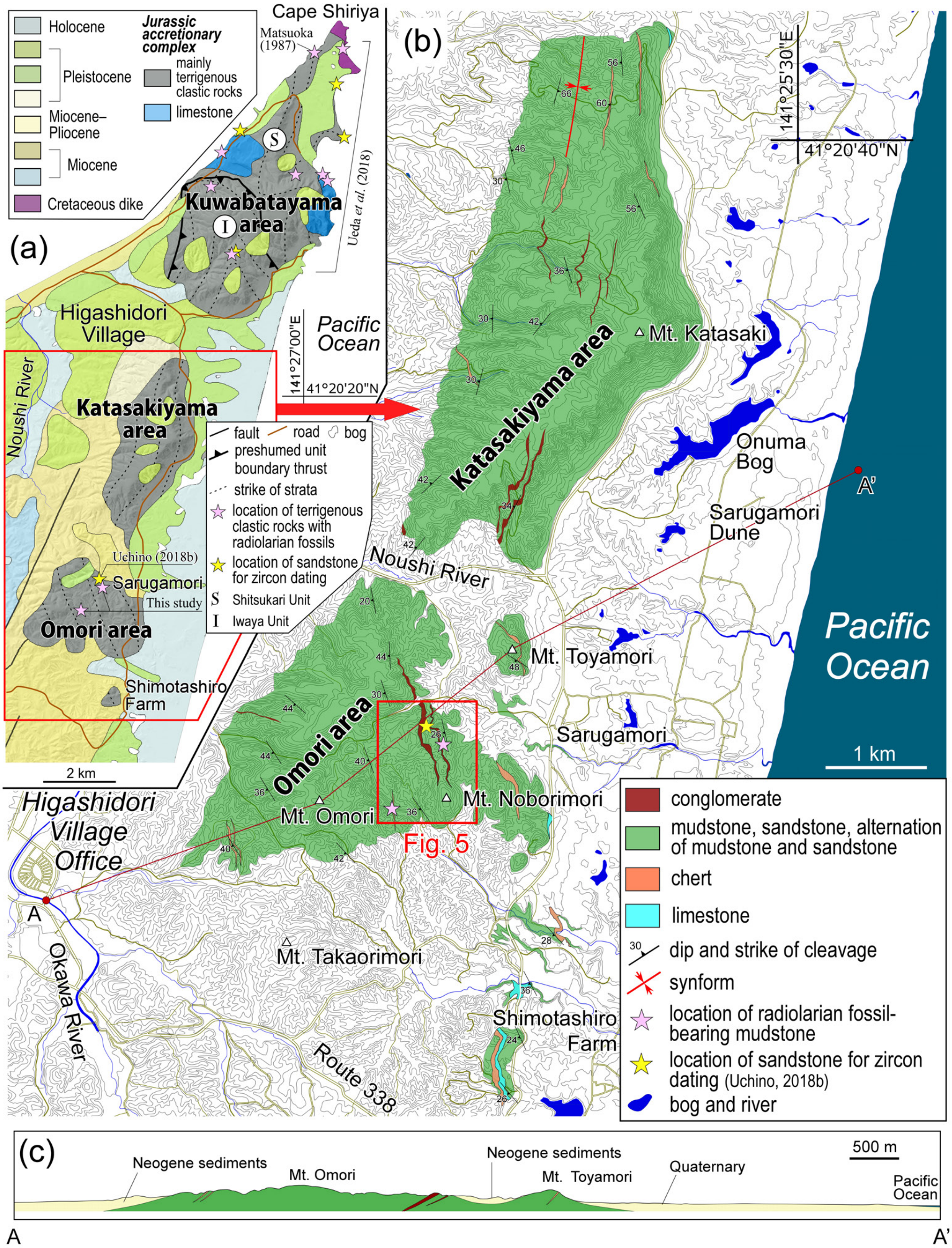

Fig. 2 (a) Index map of the northeastern Shimokita Peninsula, Aomori Prefecture. The geologic map was derived from the Seamless Digital Geological Map of Japan (1:200,000) V2 of the Geological Survey of Japan, AIST (2019). (b) Detailed geologic map of the accretionary complex in the Katasakiyama and Omori areas. The Quaternary deposits on the accretionary complexes in the two areas are not shown. (c) Geologic profile from the southwest (A) through Mt. Omori and Mt. Toyamori to the northeast (A').

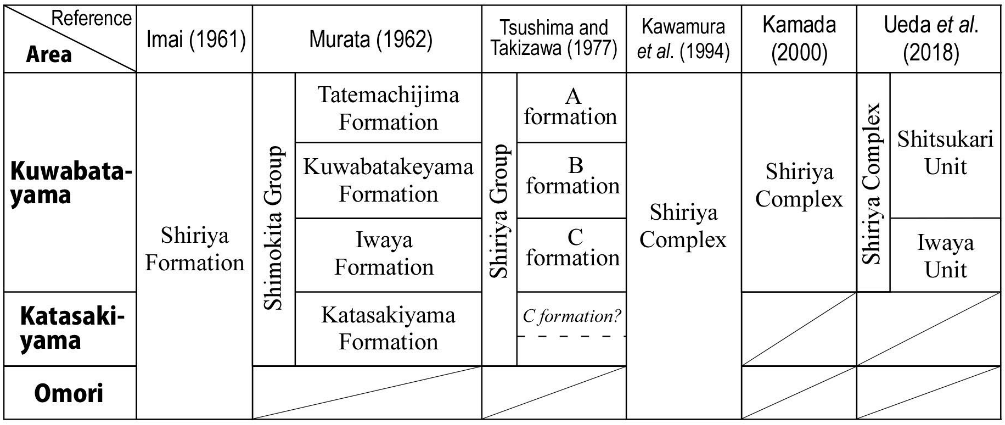

Fig. 3 Nomenclatural history of the stratigraphic units of the accretionary complexes in the northeastern Shimokita Peninsula, Aomori Prefecture. Tsushima and Takizawa (1977) indicates that the C formation in the Kuwabatayama area is probably correlative to the northern unit in the Katasakiyama area.

2. Geological outline

The North Kitakami Belt is divided into two sub-belts, namely the southwestward Kuzumaki–Kamaishi Subbelt and the northeastward Akka–Tanohata Subbelt, based on sandstone composition (dominated by plagioclase or K-feldspars), presence or absence of Paleozoic marine fossils and presence or absence of Late Jurassic coral-bearing limestone (Ehiro *et al.*, 2005; Kojima *et al.*, 2016) (Fig. 1). The AC in the Shimokita Peninsula belongs to the Akka–Tanohata Subbelt (e.g. Kamada, 2000; Ehiro *et al.*, 2008). The accretion age generally becomes younger from the southwest to the northeast (e.g. Suzuki *et al.*, 2007a; Ehiro *et al.*, 2008) although this trend does not always hold in the entire area (Nakae and Kamada, 2003). Of note, the youngest marine sediment in the North Kitakami Belt, from terrigenous clastic rocks in Cape Shiriya, was dated to the Early Cretaceous (Matsuoka, 1987; Ueda *et al.*, 2018) (Fig. 1).

2. 1 Nomenclature of stratigraphic units

The stratigraphic divisional scheme in the northeastern Shimokita Peninsula has changed over time (Imai, 1961; Murata, 1962; Tsushima and Takizawa, 1977; Kawamura *et al.*, 1994; Kamada, 2000; Kojima *et al.*, 2016; Ueda *et al.*, 2018) (Fig. 3). The pre-Neogene sedimentary rocks in this peninsula were previously thought to be "Paleozoic strata" and were named the Shiriya Formation in the 1:50,000 quadrangle series geologic map "Chikagawa" (Imai, 1961). In consideration of Mesozoic hexacorals reported from the "Paleozoic strata" in the Kuwabatayama area (Onuki, 1959), the stratigraphic divisional scheme in the northeastern Shimokita Peninsula was revised to comprise the Katasakiyama Formation in the Katasakiyama area, and the Tatemachijima, Kuwabatakeyama and Iwaya formations in the Kuwabatayama area. These four formations were grouped as the Shimokita Group (Murata, 1962). However, the name Shimokita Group was already used as a formal Miocene stratigraphic unit. Therefore, Tsushima and Takizawa (1977) renamed the four formations to the Shiriya Group. Because the strata of the North Kitakami Belt were thought to be an AC (e.g. Minoura, 1985), the Shiriya Group was renamed to the Shiriya Complex. A tectonostratigraphic continuity of this complex to the ACs of the Oshima Belt in southern Hokkaido has been found (Kawamura *et al.*, 1994). Allocation of the Shiriya Complex was expanded by Kawamura *et al.* (1994) to any ACs in the Shimokita Peninsula. Kamada (2000) confined this allocation to only the AC in the Kuwabatayama area. Recent geologic mapping, petrology, radiolarian ages and zircon U–Pb dating of the Shiriya Complex by Ueda *et al.* (2018) have led to the proposal of using the Shitsukai and Iwaya units as sub-stratigraphic units of the Shiriya Complex in the Kuwabatayama area.

We withhold specific geologic division names for the Katasakiyama and Omori areas because the first author is still engaged in a study of these areas, although the ACs in the Katasakiyama and Omori areas are likely to be correlative to the Iwaya Unit in the Kuwabatayama area, as discussed later.

2. 2 Brief overview of geology and paleontology in study areas

2. 2. 1 AC in Kuwabatayama area

The Kuwabatayama area in the present paper covers nearly the entire study areas of Murata (1962), Oho and Iwamatsu (1986), Kamada (2000), Sano *et al.* (2009) and Ueda *et al.* (2018). The Shiriya Complex (Kawamura *et al.*, 1994; Kamada, 2000) is characterized by imbricated stacks of coherent chert and clastic rock layers, and characteristic kilometer-long limestone blocks (Ueda *et al.*, 2018). The AC in Cape Shiriya is intruded by diorite 122.1+1.4 (2σ) Ma in age (Ueda *et al.*, 2018). Oho and Iwamatsu (1986) considered this AC as an olistostrome of submarine landslide deposits based on a slump with huge limestone olistoliths and the presence of a microbrecciated matrix. Recently, Ueda *et al.* (2018) divided the AC in this area into two tectonostratigraphic units (Iwaya and Shitsukari units) based on lithology and radiolarian and zircon U–Pb ages. They found that the Iwaya Unit is composed of mudstone, sandstone, chert, siliceous mudstone, and minor amounts of limestone and conglomerate. The Shitsukari Unit is composed of conglomerate, sandstone, mudstone, siliceous mudstone, chert, limestone and a minor amount of metabasalt. The Iwaya Unit, which has an approximately N–S to NW–SE trending synform, is supposed to lie structurally above the Shitsukari Unit, which has a NE–SW trending synform and antiform pair (Fig. 2a). Ueda *et al.* (2018) also found that the Shitsukari Unit formed as an imbricated accretionary wedge which was composed of debrite from an inner trench slope.

The limestone was dated to the Late Jurassic using Hexacorallia and Stromatoporoidea fossils (Onuki, 1959; Murata, 1962) and another limestone was dated to the Late Triassic using megalodontoid bivalves (Sano *et al.*, 2009). The microfossil ages of chert range from the Middle Triassic (Anisian) to the Late Jurassic (Kimmeridgian) (Toyohara *et al.*, 1980; Oho and Iwamatsu, 1986; Matsuoka, 1987; Ueda *et al.*, 2018). Siliceous mudstone yields Middle Jurassic to latest Jurassic radiolarians (Ueda *et al.*, 2018), and tuffaceous mudstone yields latest Jurassic to earliest Cretaceous radiolarians (Matsuoka, 1987). The zircon U–Pb ages of clastic rocks, including intercalated tuff layers, are correlated to the Early Cretaceous (Berriasian to Barremian) (Ueda *et al.*, 2018).

2. 2. 2 AC in Katasakiyama area

The AC in the Katasakiyama area shows a 7 km × 2.5 km lenticular distribution pattern around Mt. Katasaki. The northern part of the Katasakiyama area was partly covered by Murata (1962), who mapped a synform in the southern margin of his map. A detailed geologic map of the AC is shown in Fig. 2b, along with that in the Omori area (see next section). The AC exceeds over 1,200 m in thickness. It consists mainly of mudstone with minor amounts of chert, alternating beds of sandstone and mudstone, sandstone, conglomerate and limestone. The sheets or lens of oceanic rocks such as limestone and chert are less than several meters in thickness. The AC trends in the NNW–SSE to NNE–SSW directions and dips at a low–middle angle to the west (Fig. 2c). A thin limestone sheet several meters in thickness occurs at the northeastern edge of this area.

2. 2. 3 AC in Omori area

The AC in the Omori area shows a 2.7 km × 2.9 km elliptical distribution pattern around Mt. Omori. The thickness of the AC exceeds over 2,000 m. It consists mainly of mudstone with minor amounts of limestone, chert, alternating beds of sandstone and mudstone, sandstone and conglomerate. Similar to the limestone sheet at the northeastern edge of the Katasakiyama area, a limestone sheet <25 m in thickness is aligned, from place to place, along the eastern margin of the Omori area with a NNW–SSE trend, suggesting a possible southern extension of the limestone sheet from the Katasakiyama area. The AC trends in the NW–SE to NNW–SSE directions and dips at a low–middle angle to the west (Fig. 2b, c).

3. Lithology

The lithologies of the ACs in the Katasakiyama and Omori areas are very similar and are thus described collectively in this section. That in the Kuwabatayama area is not explained here because it has been described in previous reports.

Limestone, which accounts for ca. 0.4 % of the mapped distribution area of the AC, is gray to pale gray and mostly recrystallized. Macroscopic and microscopic calcite veins less than 1 cm in width frequently crosscut the limestone, and some of them are dark pink. Matrix-supported and poorly sorted calcirudite infrequently occurs with preserving as an original sedimentary structure. The limestone clasts in the calcirudite do not exceed 4 cm in length. Chert, which accounts for ca. 1 % of the mapped distribution area, is gray. It has a bedded structure, where several-centimeter-thick chert layers alternate with ca. 1-mm-thick claystone layers. The chert is mostly recrystallized. Dark gray mudstone is the most dominant rock type in the AC. The mudstone is more or less slaty, and frequently contains radiolarian fossil pseudomorphs. Quartz veins less than 1 cm in width occasionally intrude into the mudstone.

Sandstone, which accounts for a ca. 1 % of the mapped distribution area, occurs as feldspathic arenite (Fig. 4a) and lithic arenite to wacke. Quartz grains are more common than feldspar ones, which have nearly equal amounts of plagioclase and K-feldspar. This sandstone varies from fine to very coarse grains and is in general poorly sorted. It also contains many lithic fragments such as chert and siliceous mudstone, and frequently contains contemporaneous mud chips. It is occasionally intruded by quartz veins less than 5 cm in width. The sandstone sometimes alternates with mudstone in the form of layers with a thickness on the order of several millimeters. Rarely, pale purple tuffaceous sandstone appears.

Poorly sorted, granule to pebbly conglomerates (Fig. 4b, c) account for 1 % of the mapped distribution area of the AC in these two areas. They are mostly characterized by a clast-supported fabric with coarse quartz grains, angular to sub-rounded variable clasts of chert (gray, dark gray, white and rarely red), siliceous mudstone, mudstone and sandstone.

These sedimentary rocks have undergone extensive post-depositional alteration and deformation, with layer-parallel slaty cleavage in the fissile mudstone and considerably flattened clasts in the conglomerate (Fig. 4c). The mudstone sometimes exhibits whitish parts caused by

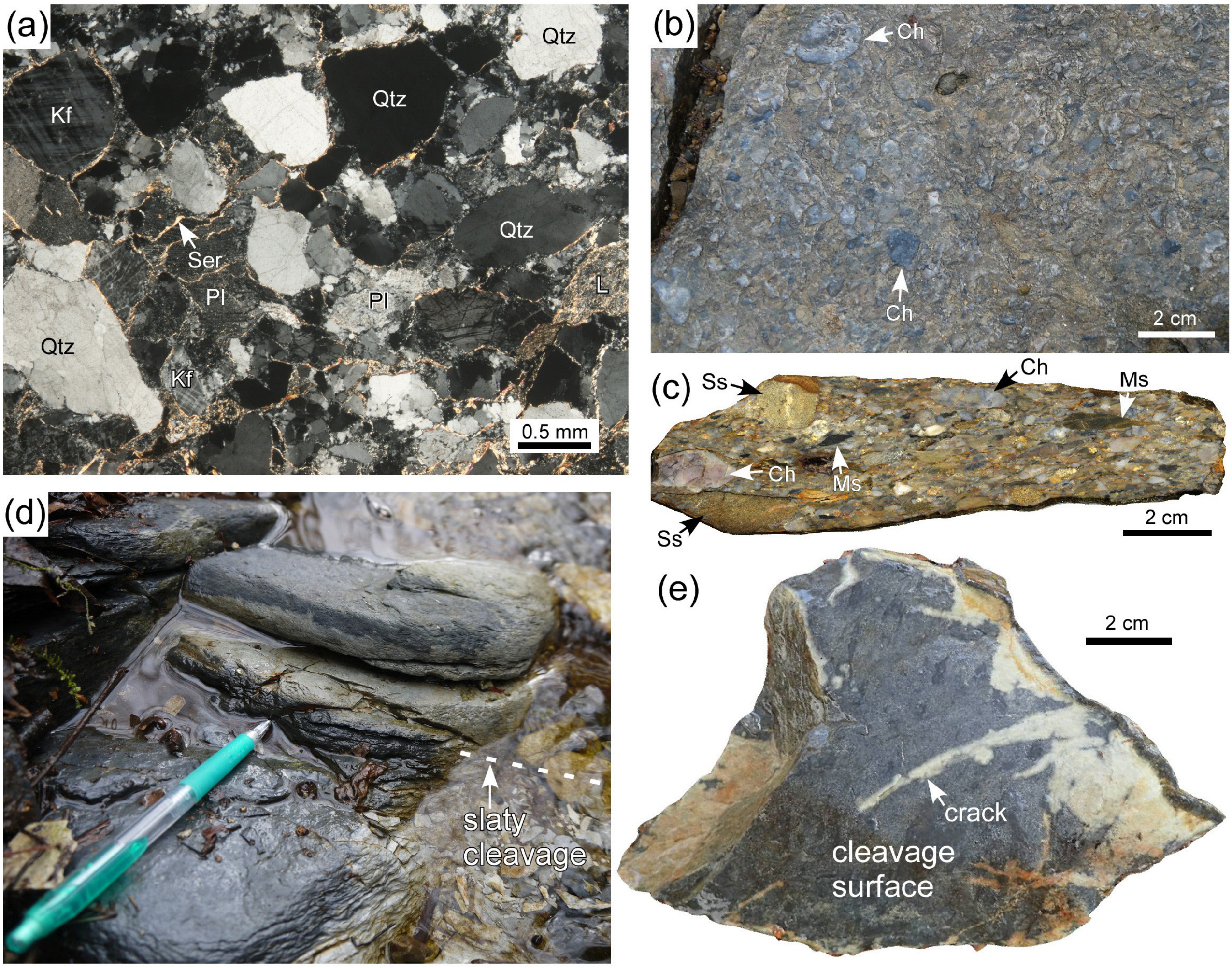

Fig. 4 (a) Photomicrograph of feldspathic arenite. Cross-polarized light. Mizunashi Stream, east ramp of Mt. Katasaki. Kf: K-feldspar, Pl: plagioclase, Qtz: quartz, Ser: sericite, L: lithic fragment (mudstone). (b) Conglomerate outcrop. Stream to the west of Sarugamori hamlet. Ch: chert. (c) Conglomerate specimen. Ch: chert, Ms: mudstone, Ss: sandstone. (d) Altered mudstone outcrop. The pen is 15 cm long. (e) Altered mudstone specimen. Stream to the west of Mt. Toyamori.

fluid flow along the slaty cleavages and cracks, and looks as if it was tuffaceous or calcareous mudstone (Fig. 4d, e). Fine clay minerals such as sericite, which are mostly in a unidirectional polarization extinction position, are found between the clastic grains (Fig. 4a). Very fine ferric oxyhydroxide minerals frequently develop along the cleavages and cracks or between the clastic grains. Calcite spots (<0.2 mm in diameter) that are not aligned with the cleavages are occasionally present in the clastic rocks, and quartz spots (<0.2 mm) containing very fine dusty inclusions appear in the matrix of limestone and calcite veins.

4. Radiolarian fossil

4. 1 Sample location and extraction method

Samples containing radiolarian fossils were recovered from mudstone at two outcrops in the stream: Loc. 1 (41°17′05″N, 141°22′35″E) ca. 550 m west and Loc. 2 (41°17′25″N, 141°22′56″E) ca. 550 m north of Mt. Noborimori (Fig. 2b). The mudstone is dark gray and does not exhibit the apparent deformation or alteration. A route map and a columnar section around these outcrops are shown in Figs. 5 and 6, respectively. Of note, Loc. 2 is close to an outcrop of the Late Jurassic sandstone dated using detrital zircon U–Pb geochronology (Uchino, 2018b).

Rock chips were soaked in 5 % HF for ca. 18 hours and then residual fractions were collected with sieves of #65 and #250 meshes. After these steps were repeated three times, radiolarian samples were picked with a brush under a stereomicroscope and subsequently examined with a scanning electron microscope.

Regarding taxonomy, the species was determined by strictly referring to the holotype or other type series images in original publications, and the genus was determined by

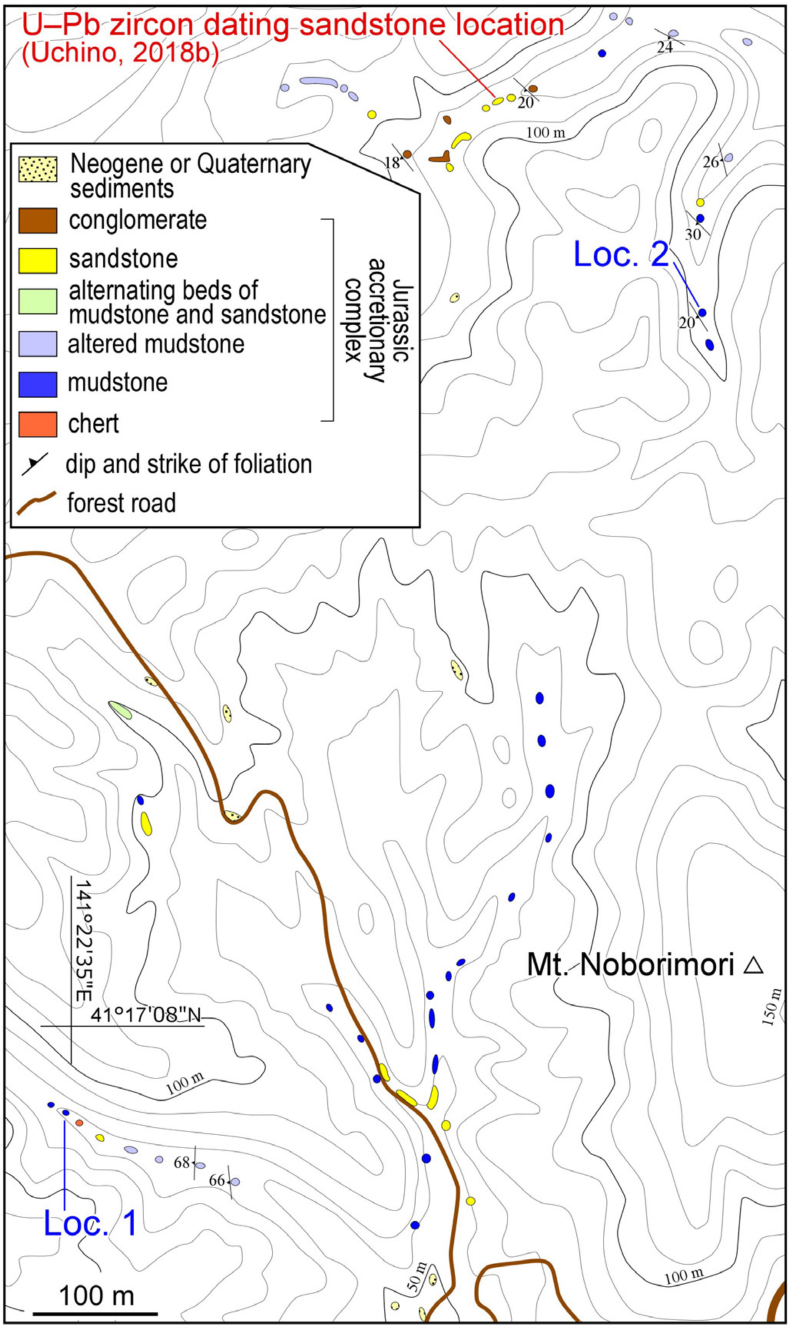

Fig. 5 Route map around the location of radiolarian fossil-bearing mudstone. Contour lines were derived from digital elevation model data (10-m mesh) from the Geospatial Information Authority of Japan.

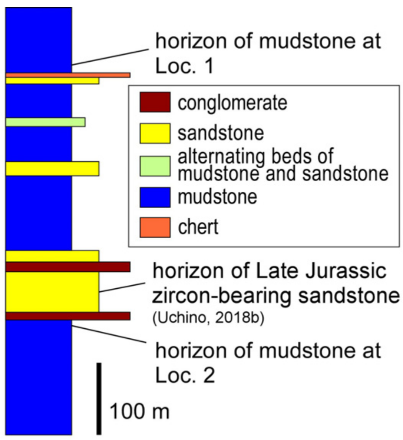

Fig. 6 Columnar section around the location of radiolarian fossil-bearing mudstone.

referring to updated concepts if possible (e.g. O'Dogherty *et al.*, 2017). The biostratigraphic correlation to the geologic time scale at the stage level was largely based on the Jurassic standard radiolarian zones proposed by Matsuoka (1995) and some revisions in subsequent papers (Hatakeda *et al.*, 2007; Ishida *et al.*, 2009). Because of a contradiction in the denoted geologic stages of the same fauna among Japan, Europe and North America, the assigned geologic time scale was converted from biozones in other regions to those of Japan by referencing Baumgartner *et al.* (1995), Yang and Matsuoka (1997) and Goričan *et al.* (2018).

4. 2 Identification and age

4. 2. 1 Radiolarians at Loc. 1

Many of the radiolarian fossils were deformed and recrystallized. Although their surface structure is hard to be recognized, 33 species or species levels are identified.

Table 1 List of radiolarian fossils. Red and blue numbers indicate individuals from the mudstone at Loc. 1 and Loc. 2, respectively.

Fossil	Loc. 1	Loc. 2	Individual number in plate
Archaeodictyomitra cf. *inornata* Hull	*	*	21–23, 4
Archaeodictyomitra cf. *unica* Wu	*		15
Archaeodictyomitra aff. *prisca* Kozur and Mostler in Grill and Kozur (1986)	*		7
Archaeodictyomitra aff. *rigida* Pessagno	*	*	16, 17, 1, 2
Archaeodictyomitra spelae Chiari, Cortese and Marcucci	*		1–3
Archaeodictyomitra cf. *spelae* Chiari, Cortese and Marcucci	*		4–6
Archaeodictyomitra aff. *suzukii* Aita	*		18–20
Archaeodictyomitra cf. *tyaughtonensis* Cordey		*	3
Archaeodictyomitra aff. *vulgaris* Pessagno	*		11–14
Archaeodictyomitra sp. A	*		8
Archaeodictyomitra sp. B	*		9, 10
Archaeodictyomitra sp. C	*		24
Archaeodictyomitra sp. D	*		25
Archaeospongoprunum cf. *mizutanii* Ožvoldová in Ožvoldová *et al.* (2000)	*		109
Archaeospongoprunum sp.	*		108
Bistarkum aff. *mangartense* Goričan, Šmuc and Baumgartner	*		112, 113
Cinguloturris cf. *carpatica* Dumitrică in Dumitrică and Mello (1982)	*	*	38–43, 17
Cinguloturris cf. *floridicingula* (Li)		*	15
Cinguloturris cf. *getsensis* O'Dogherty, Goričan and Dumitrică in O'Dogherty *et al.* (2006)		*	16
Cinguloturris cf. *latiannulatum* (Grill and Kozur)	*		44
Cinguloturris sp.	*		45
Crococapsa aff. *truncata* (Wu)	*		63
Eucyrtidiellum cf. *nodosum* Wakita	*		62
Eucyrtidiellum cf. *pyramis* (Aita) in Aita and Okada (1986)	*		59–61
Eucyrtidiellum sp.		*	29
Favosyringium cf. *affine* (Rüst) sensu Steiger (1992)	*		111
Kilinora sp.	*		69
Loopus cf. *venusta* (Chiari, Cortese and Marucci)	*		37
Minutosolla sp.	*		88, 89
Parahsuum mudongensis (Li) sensu lato	*		26–28
Podobursa sp.	*		110
Praewilliriedellum sp.	*		78
Hiscocapsa robusta (Matsuoka)	*		91, 92
Hemicryptocapsa cf. *yaoi* (Kozur)	*		93
Hemicryptocapsa carpathica (Dumitrică)	*		79
Praezhamoidellum sp.	*		94–98
Praezhamoidellum ? sp.	*		90
Quarkus sp.		*	30
Spongocapsula palmerae Pessagno	*		29–31
Spongocapsula sp.	*		32, 33
Spongocapsula ? sp.	*		34–36
Striatojaponocapsa cf. *conexa* (Matsuoka)	*		70
Striatojaponocapsa synconexa O'Dogherty, Goričan and Dumitrică in O'Dogherty *et al.* (2006)	*		71–76
Striatojaponocapsa sp.	*		77
Svinitzium sp.	*		46, 47
Tetracapsa sp.		*	31
Transhsuum sp.	*		49–55
Wrangellium sp.	*		48
Williriedellum sp.	*	*	80–87, 20–23
Complexapora aff. *kiesslingi* Hull	*		105, 106
Zhamoidellum cf. *mikamense* Aita		*	19
Zhamoidellum ovum Dumitrică	*		101–104
Zhamoidellum cf. *ventricosum* Dumitrică	*		100
Zhamoidellum sp.	*		99
Minocapsidae gen. et sp. indet.	*		107
Pyloniodea gen. et sp. indet.	*		58
Multisegmented nassellarians		*	5–14
Spherical radiolarians		*	18
Williriedelloidea gen. et sp. indet.		*	24–26
Syringocapsidae? gen. et sp. indet.		*	27, 28
Few segmented nassellarians		*	32–35
Four-armed flat Pylonioidea		*	36
Nassellaria gen. et sp. indet.	*		56, 57, 64–68, 114

A total of approximately 15 species coexisted in the early to middle Late Jurassic (roughly Oxfordian or Kimmeridgian): *Archaeodictyomitra* cf. *inornata* Hull, *Archaeodictyomitra* cf. *unica* Wu, *Archaeodictyomitra spelae* Chiari *et al.* (a single report from the Oxfordian), *Archaeospongoprunum* cf. *mizutanii* Ožvoldová [known from Oxfordian and Tithonian], *Cinguloturris* cf. *carpatica* Dumitrică, *Cinguloturris* cf. *latiannulatum* (Grill and Kozur), *Eucyrtidiellum* cf. *nodosum* Wakita, *Eucyrtidiellum* cf. *pyramis* (Aita) (Kimmeridgian and later), *Loopus* cf. *venusta* (Chiari *et al.*), *Parahsuum mudongensis* (Li) sensu lato, *Hiscocapsa robusta* (Matsuoka), *Hemicryptocapsa* cf. *yaoi* (Kozur), *Spongocapsula palmerae* Pessagno, *Striatojaponocapsa* cf. *conexa* (Matsuoka), *Hemicryptocapsa carpathica* (Dumitrică), *Zhamoidellum ovum* Dumitrică, and *Zhamoidellum* cf. *ventricosum* Dumitrică. By contrast, 12 species, such as *Striatojaponocapsa synconexa* O'Dogherty *et al.*, are referable to the late Middle Jurassic (roughly Callovian). Eight species are common in the late Late Jurassic (Tithonian). These eight species, however, range down to the middle Late Jurassic (Kimmeridgian), and are thus not necessarily from the Tithonian. Therefore, the fauna from Loc. 1 is roughly dated to the early to middle Late Jurassic. Based on species whose ranges are well documented (Aita, 1987; Matsuoka, 1995; Nishizono, 1996; Hori, 1999; Hatakeda *et al.*, 2007), the co-occurrence of *Striatojaponocapsa* cf. *conexa* (Matsuoka) and *Striatojaponocapsa synconexa* O'Dogherty *et al.* is correlative to JR5 (*S. conexa* Zone) to JR6 (*Kilinora spiralis* Zone) of Matsuoka (1995). These two zones are generally correlated to the Bathonian and Callovian. However, Ishida *et al.* (2009) reported the earliest Kimmeridgian ammonoid, *Ataxioceras* (*Ataxioceras*) *kurisakense*, from bioturbated sandy mudstone 1.5 m above the horizon of the JR6 fauna with *S. conexa* and *S. synconexa* (= *Stichocapsa naradaniensis* Matsuoka shown in Fig. 7.9 of Ishida *et al.*, 2009) from the Kurisaka Formation of the Kurosegawa Belt in Shikoku, Southwest Japan. This suggests that an extension of geologic time ranges up to the earliest Kimmeridgian from the Callovian, or an age revision from the Callovian to a significantly younger age is needed. The contradiction of ranges of the radiolarian zone shown by Matsuoka (1995) was pointed out for stratigraphically important *Kilinora spiralis*, *Loopus primitivus* (Matsuoka and Yao), *Striatojaponocapsa plicarum* (Yao) and *S. conexa* by Hori *et al.* (2002). Because the occurrence of *S. conexa* and *S. synconexa* can also be explained by reworking to the lowest Kimmeridgian strata, we focus on *Eucyrtidiellum* cf. *pyramis*, whose ranges are the youngest among the fauna from Loc. 1. The genus *Eucyrtidiellum* is composed of 19 species. The form of *E. pyramis* is quite distinctive, with widely spaced longitudinal plicae on both the thorax and abdomen and a smooth cone shape, from any other *Eucyrtidiellum* species. The first occurrence of *E. pyramis* was correlative to the radiolarian *Ditrabs sansalvadorensis* Zone of Aita (1987) and UAZ 12 of Baumgartner *et al.* (1995), indicating the Tithonian according to Aita (1987) and Goričan *et al.* (2018). The oldest occurrence of *E. pyramis* is from the Nusplingen Lithographic Limestone in Germany, which yielded late Kimmeridgian ammonoids indicative of the *Lithacoceras ulmense* Subzone of Zügel *et al.* (1998). Although it is unclear why *E.* cf. *pyramis*, *S.* cf. *conexa* and *S. synconexa* co-exist in the same sample, the sample can be roughly dated to the Kimmeridgian (157.3±1.0 Ma to 152.1±0.9 Ma).

4. 2. 2 Radiolarians at Loc. 2

Radiolarian fossils at Loc. 2 were more deformed and recrystallized than those at Loc. 1. Their surface structure was difficult to identify. A total of 11 taxa at the genus or species level were identified in this sample. Identified taxa at the species level are *Archaeodictyomitra* cf. *inornata*, *Archaeodictyomitra* aff. *rigida*, *Archaeodictyomitra* cf. *tyaughtonensis* Cordey, *Cinguloturris* cf. *carpatica*, *Cinguloturris* cf. *floridicingula* (Li), *Cinguloturris* cf. *getsensis* O'Dogherty *et al.* and *Zhamoidellum* cf. *mikamense* Aita. Although three of these seven species (*A*. cf. *inornata*, *A*. aff. *rigida* and *C*. cf. *carpatica*) were also found at Loc. 1, they are generally dated to the late Middle Jurassic (probably Callovian) to middle Late Jurassic (probably Kimmeridgian). There were no taxa that could be certainly assigned to a geologic age later than this suggested age. It was impossible to determine ages at higher resolution. Most of these species (e.g. *A*. cf. *tyaughtonensis*) are rarely reported after their first description or they cannot be used for age determination. For example, *Cinguloturris carpatica* belongs to the latter case. It is subdivided into several *Cinguloturris* species, such as *C. floridicingula* and *C. getsensis*. *Zhamoidellum mikamense* was combined with *Zhamoidellum ovum* Dumitrică as a junior synonym (Baumgartner *et al.*, 1995). Thus, taxonomic confirmation of these two species is needed to determine the precise age. In consideration of the insufficient number of reports for the rare taxa and incomplete updating of the taxonomic concept of age-index species, we retain the radiolarian age for the Loc. 2 sample as the late Middle Jurassic (probably Callovian) to middle Late Jurassic (probably Kimmeridgian).

5. Discussion

5. 1 Depositional age of clastic rocks

The youngest cluster U–Pb ages of detrital zircon from sandstone in the Omori area are 154.7±1.5 Ma (1σ) and 155.6±3.2 Ma (2σ), obtained using different calculation methods (Uchino, 2018b). These ages correspond to the latest Oxfordian–Kimmeridgian under the geologic time scale of Cohen *et al.* (2013). A detrital zircon age suggests only a possible lower limit of a depositional age of sandstone, although the zircon age can approximate the depositional age if volcanism in its hinterland was very active. However, volcanism in eastern Asia, including the paleo-Japanese islands, was not very active during the Late Jurassic–earliest Cretaceous (e.g. Sagong *et al.*, 2005; Kiminami and Imaoka, 2013; Lee *et al.*, 2018). The low age spectrum peak of the youngest cluster of the detrital zircon from the sandstone in the Omori area shown by Uchino (2018b) probably reflects this weak volcanism in the hinterland. Therefore, the sandstone was deposited in the latest Oxfordian–Kimmeridgian or later.

The radiolarian fossil age from mudstone can directly indicate the depositional age of the mudstone if the fossils were not reworked. In consideration of the reliability of the assigned radiolarian ages for the mudstone at Locs. 1 and 2, the mudstone ages of the Kimmeridgian at Loc. 1 and the late Middle Jurassic (probably Callovian) to middle Late Jurassic (probably Kimmeridgian) at Loc. 2 are close to the U–Pb age of the sandstone in the Omori area. In addition, the horizons of the mudstone and sandstone are close to each other without any recognizable distinctive tectonic discontinuity between them (Figs. 5, 6), indicating that these clastic rocks may be stratigraphically continuous or contemporaneous sequences. Therefore, the clastic rocks in the Omori area were deposited in a trench around the Kimmeridgian (middle Late Jurassic).

5. 2 Tectonostratigraphic correlation

The ACs identified in the Shimokita Peninsula are, from north to south, the Shiriya Complex (the Iwaya and Shitsukari units) in the Kuwabatayama area, an unnamed AC in the Katasakiyama area and an unnamed AC in the Omori area. Tsushima and Takizawa (1977) pointed out that the Iwaya Unit (“C formation” in the original paper) of the Shiriya Complex in the Kuwabatayama area is similar to the northernmost part of the AC in the Katasakiyama area (Fig. 3). In consideration of the trends in geologic structures, such as the NE–SW strikes of the Shitsukai Unit in the northern Kuwabatayama area, the N–S to NW–SE strikes of the Iwaya Unit in the southern Kuwabatayama area, the NNE–SSW to NNW–SSE strikes of the AC in the Katasakiyama area and the NW–SE to NNW–SSE strikes in the Omori area, the Iwaya Unit in the Kuwabatayama area and the ACs in the Katasakiyama and Omori areas are presumably tectonically continuous (Fig. 2a).

According to Ueda *et al.* (2018) and other previous papers, the Iwaya Unit differs from the Shitsukari Unit in that the latter exclusively contains basalt, huge limestone blocks and lithic sandstone, and is characterized by slump facies indicating debrite (Figs. 2a, 3). In addition, the age of the clastic rocks in the Iwaya Unit is the Late Jurassic, younger than the Early Cretaceous age of the clastic rocks in the Shitsukai Unit.

The lithologies of the ACs in the Katasakiyama and Omori areas are more similar to that in the Iwaya Unit than that in the Shitsukai Unit, in particular in terms of the presence of characteristic quartzo-feldspathic sandstone (Fig. 4a) and small amounts of limestone and conglomerate. The assigned age of the Kimmeridgian (the Late Jurassic) to the clastic rocks of the AC in the Omori area overlaps the age of the Iwaya Unit in the southern Kuwabatayama area, which supports the probable tectonostratigraphic continuity of the ACs in the Katasakiyama and Omori areas to the Iwaya Unit in the Kuwabatayama area.

Although more detailed studies are needed to confirm this assumption, the ACs in the northeastern Shimokita Peninsula are likely to comprised a Late Jurassic tectonostratigraphic unit and an overlain Early Cretaceous unit. The former is the Iwaya Unit in the southern Kuwabatayama area and the unnamed ACs in the Katasakiyama and Omori areas, and the latter is the Shitsukari Unit, which has only been found in the northern Kuwabatayama area so far.

5. 3 Younging polarity

It has been reported that a younging polarity of accretion ages for trench-fill terrigenous clastic rocks in the North Kitakami Belt is detectable from the southwest to the northeast, in a direction perpendicular to the general NW–SE to NNW–SSE distribution trends of the ACs in the belt (e.g. Suzuki *et al.*, 2007a; Ehiro *et al.*, 2008; Kojima *et al.*, 2016) (Figs. 1, 7). The geologic columns of the ocean plate stratigraphy reconstructed in each area are compiled in Fig. 7, although the terms “complex” and “unit” are mixed in the figure. The depositional ages of terrigenous rocks within the ACs in the “B” zone of Otoh and Sasaki (2003) range from the Late Triassic in the Kadoma Complex (Uchino, 2017), through the Early Jurassic in the Nishimatayama Unit and the Nakatsugawa Complex (Ueda *et al.*, 2009; Uchino, 2019), to the Middle Jurassic in the Shibamori Complex, possibly the Nakatsugawa Complex, and the Tsugaruishi Unit (Yoshihara *et al.*, 2002; Suzuki and Ogane, 2004; Suzuki *et al.*, 2007a; Uchino, 2018a; Uchino, 2019). No age data for the trench-fill terrigenous rocks has been reported in the “C” zone excluding the Late Jurassic coral fossils from possible shallow marine deposits. The “D” and “E” zones range from the Middle Jurassic to the Late Jurassic in the Kado–Akka areas (Nakae and Kamada, 2003; Suzuki *et al.*, 2007b; Ehiro *et al.*, 2008).

The “B”–“E” zones belong to the Kuzumaki–Kamaishi Subbelt, and the “A” zone belongs to the Nedamo Belt. The Akka–Tanohata Subbelt fully corresponds to the “F” and “G” zones, whose depositional ages range from the Middle–Late Jurassic in the Takayashiki and Magisawa units (Minoura and Tsushima, 1984; Matsuoka and Oji, 1990; Suzuki *et al.*, 2007a), through the Late Jurassic in the Iwaya Unit and its equivalent (Matsuoka, 1987; Ueda *et al.*, 2018; this study), to the late Late Jurassic to the early Early Cretaceous in the Shitsukari Unit (Matsuoka, 1987; Ueda *et al.*, 2018). The present study confirmed that the Late Jurassic ACs in the northeastern Shimokita Peninsula are distributed in the Kuwabatayama area as the Iwaya Unit and in the Omori area as an unnamed AC, and probably in the Katasakiyama area as an unnamed AC.

A well-ordered younging polarity was found in the

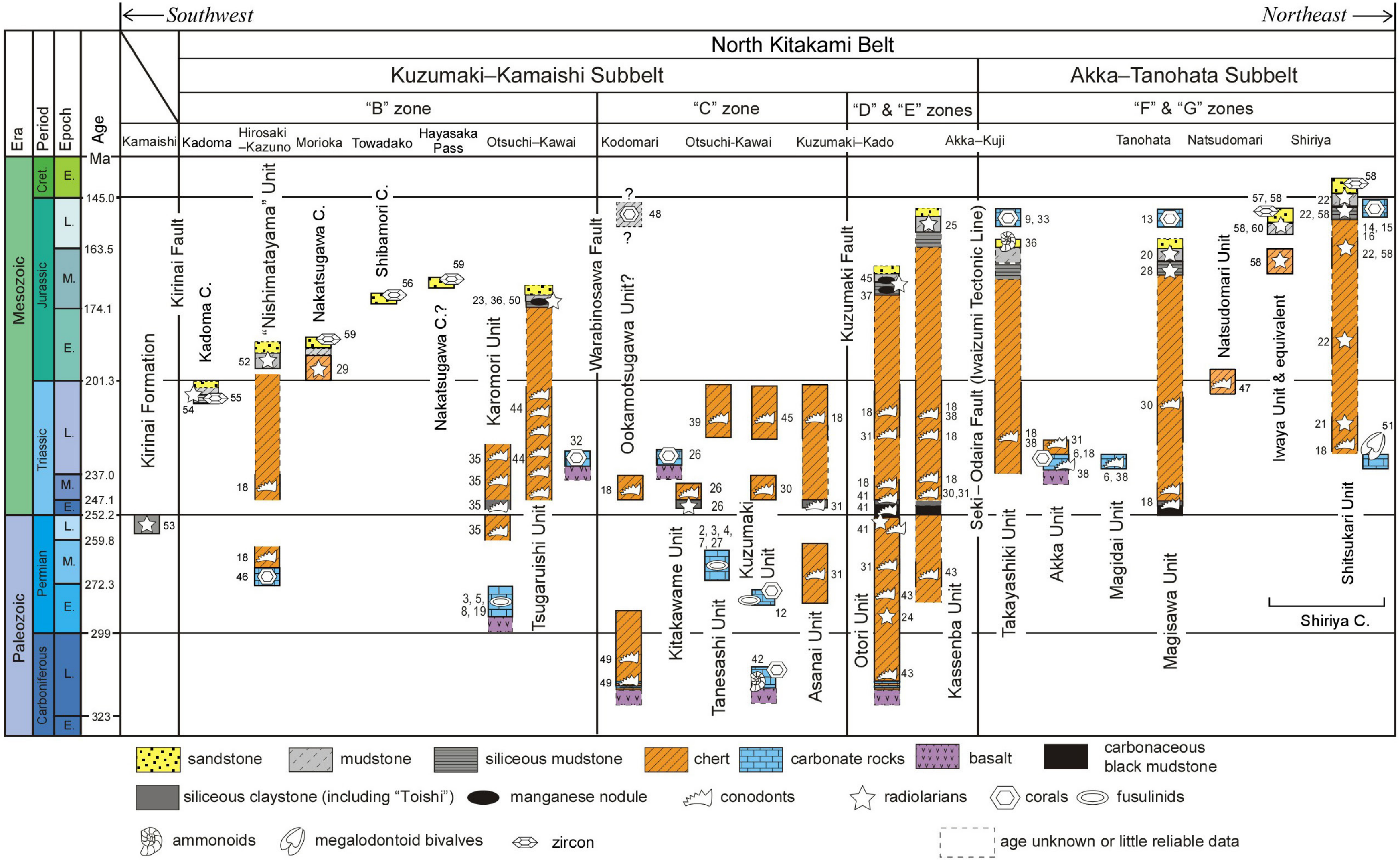

Fig. 7 Schematic compilation diagram of age and lithostratigraphic column of the North Kitakami Belt. This diagram was revised based on Fig. 42 of Suzuki *et al.* (2007a), Fig. 3 of Ehiro *et al.* (2008) and Fig. 2b. 41 of Kojima *et al.* (2016). Numbers beside fossil and zircon symbols correspond to literature references. See Suzuki *et al.* (2007a) for nos. 1–35 and Ehiro *et al.* (2008) for nos. 36–45. 46: Fujimoto and Kobayashi (1961), 47: Murata and Nagai (1972), 48: Kato (1972), 49: Murata *et al.* (1974), 50: Yoshihara *et al.* (2002); 51: Sano *et al.* (2009), 52: Ueda *et al.* (2009), 53: Nakae and Kurihara (2011), 54: Kawamura *et al.* (2013), 55: Uchino (2017), 56: Uchino (2018a), 57: Uchino (2018b), 58: Ueda *et al.* (2018), 59: Uchino (2019), 60: this study. See Otoh and Sasaki (2003) for "A"–"G" zones. L.: Late, M.: Middle, E.: Early, C.: Complex. Tectonostratigraphic names are taken from the original papers or Fig. 2b. 41 of Kojima *et al.* (2016), and the appropriateness of the terms "complex" and "unit" are not discussed in the present paper.

Kuzumaki–Kamaishi Subbelt. By contrast, the age polarity in the Akka–Tanohata Subbelt appears somewhat disordered, as shown in Fig. 7. Possible reasons for this disorder include wrong reconstruction of complexes/units, no age data for the terrigenous clastic rocks of the Magidai Unit in the Tanohata area, and repeated distribution of the same tectonostratigraphic units by folding or out-of-sequence thrust. Despite this, when viewing the younging polarity from a broad perspective, the trend from the Late Triassic of the southwesternmost AC (Kadoma Complex) of the Kuzumaki–Kamaishi Subbelt to the early Early Cretaceous of the northeasternmost AC (Shitsukari Unit of the Shiriya Complex) of the Akka–Tanohata Subbelt is well constrained in the North Kitakami Belt based on the data in this study.

6. Conclusion

Radiolarian fossils from around the Kimmeridgian (middle Late Jurassic) were extracted from mudstone in the AC in the Omori area, northeastern Shimokita Peninsula. The ACs in the Kasakiyama and Omori areas are correlative to the Iwaya Unit, the southern unit in the Kuwabatayama area, based on the lithology, geologic structure and clastic rock ages.

Acknowledgments:We are grateful to Dr. Kamata, Y. (University of Tsukuba) for reviewing the manuscript.

References

Aita, Y. (1987) Middle Jurassic to Lower Cretaceous radiolarian biostratigraphy of Shikoku with reference to selected sections in Lombardy basin and Sicily. *The Science Reports of the Tohoku University, Second Series (Geology)*, **58**, 1–91.

Aita, Y. and Okada, H. (1986) Radiolarians and calcareous nannofossils from the uppermost Jurassic and Lower Cretaceous strata of Japan and Tethyan regions. *Micropaleontology*, **32**, 97–128.

Baumgartner, P. O., Bartolini, A., Carter, E. S., Conti, M., Cortese, G., Danelian, T., DeWever, P., Dumitrica, P., Dumitrica-Jud, R., Gorican, S., Guex, J., Hull, D. M., Kito, N., Marcucci, M., Matsuoka, A., Murchey, B., O'Dogherty, J., Savaray, J.,Vishnevskaya, V.,Widz, D. and Yao, A. (1995) Middle Jurassic to Early Cretaceous radiolarian biochronology of Tethys based on UnitaryAssociations. *Memories de Geologie (Lausanne)*, no. 23, 1013–1048.

Cohen, K. M., Finney, S. C., Gibbard, P. L. and Fan, J. -X. (2013) The ICS International Chronostratigraphic Chart. *Episodes*, **36**, 199–204.

Dumitrică, P. and Mello, J. (1982) On the age of the Meliata Group and the Silica Nappe radiolarites (localities Držkovce and Bohúňovo, Slovak Karst, ČSSR). *Geologické Práce,* **77**, 17–28.

Ehiro, M., Kawamura, M. and Kawamura, T. (2005) *Appendix for the Geology of Japan: General Geology and Divisions, Meso–Paleozoic of the Tohoku district*. 49–50, Kyoritsu Publishing, Tokyo (in Japanese).

Ehiro, M., Yamakita, S., Takahashi, S. and Suzuki, N. (2008) Jurassic accretionary complexes of the North Kitakami Belt in the Akka–Kuji area, Northeast Japan. *The Journal of the Geological Society of Japan*, **114** Supplement, 121–139 (in Japanese).

Fujimoto, H. and Kobayashi, F. (1961) On the Paleozoic deposites of the Inner Zone of the Ou region. *The Journal of the Geological Society of Japan*, **67**, 221–227 (in Japanese with English abstract).

Geological Survey of Japan, AIST (2019) *Seamless Digital Geological Map of Japan (1:200,000) V2*, https://gbank.gsj.jp/seamless/ (Accessed: 2019-02-14).

Goričan, S., O'Dogherty, L., Baumgartner, P. O., Carter, E. S. and Matsuoka, A. (2018) Mesozoic radiolarian biochronology – current status and future directions. *Revue de Micropaléontologie*, **61**, 165–189.

Grill, J. and Kozur, H. (1986) The first evidence of the *Unuma echinatus* radiolarian zone in the Rudabanya Mts. (Northern Hungary). *Geologisch-Paläontologische Mitteilungen Innsbruck*, **13**, 239–275.

Hatakeda, K., Suzuki, N. and Matsuoka, A. (2007) Quantitative morphological analyses and evolutionary history of the Middle Jurassic polycystine radiolarian genus *Striatojaponocapsa* Kozur. *Marine Micropaleontology*, **63**, 39–56.

Hori, N. (1999) Latest Jurassic radiolarians from the northeastern part of the Torinoko Block, Yamizo Mountains, central Japan. *Science Reports of the Institute of Geoscience, University of Tsukuba, Section B: Geological Sciences*, **20**, 27–114.

Hori, N., Saito, M. and Toshimitsu, S. (2002) Late Jurassic radiolarian fauna from the Ikenohara Formation of the Kurosegawa Belt in the Toyo-Izumi area, Kumamoto Prefecture, Kyushu, Japan. *Bulletin of the Geological Survey of Japan*, **69**, 37–46.

Imai, I. (1961) *Geological Sheet Map 1:50,000 "Chikagawa"*, Geological Survey of Japan. 45p (in Japanese with English abstract).

Ishida, K, Tsujino, Y, Kozai, T, Sato, T. and Hirsch, F. (2009) Direct correlation of radiolarian *Kilinora spiralis* Zone with the Late Jurassic ammonite faunal succession in the Kurisaka Formation, Kurosegawa Terrane, SW Japan. *Science in China Series D Earth Sciences*, **52**, 1910–1923.

Kamada, K. (2000) Shiriya Complex: Pre-Tertiary accretional complex at Cape Shiriya, northern Japan. *Bulletin of the Faculty of Education, Hirosaki University*, **83**, 39–47 (in Japanese with English abstract).

Kato, M. (1972) "Paleozoic strata" in the Tsugaru Peninsula, Aomori Prefecture. *The Journal of the Geological Society of Japan*, **78**, 515 (in Japanese).

Kawamura, M., Otsu, S., Terada, T. and Yasuda, N. (1994) Geology and internal structure of the Oshima accretionary complex. *Field Trip Guidebook, 101st Annual Meeting of Geological Society of Japan*, 175–195, Nakanishi Printing Office, Sapporo (in Japanese).

Kawamura, T., Uchino, T. and Kawamura, M. (2013) Chapter 8, Jurassic of the North Kitakami Terrane, *Geology of the Hayachine San District*. Quadrangle Series, 1:50,000, Geological Survey of Japan, AIST, 62–67 (in Japanese with English abstract).

Kiminami, K. and Imaoka, T. (2013). Spatiotemporal variations of Jurassic–Cretaceous magmatism in eastern Asia (Tan-Lu Fault to SW Japan): Evidence for flat-slab subduction and slab rollback. *Terra Nova*, **25**, 414–422.

Kojima, S., Hayasaka, Y., Hiroi, Y. Matsuoka, A., Sano, H., Sugamori, Y., Suzuki, N., Takemura, S., Tsujimori T. and Uchino, T. (2016) 2b Pre-Cretaceous accretionary complexes. *In* Moreno, T., Wallis, S., Kojima, T. and Gibbons, W., eds., *The Geology of Japan*, Geological Society of London, 61–100.

Lee, T.-H., Park, K.-H. and Yi, K. (2018) SHRIMP U–Pb ages of detrital zircons from the Early Cretaceous Nakdong Formation, south east Korea: Timing of initiation of the Gyeongsang Basin and its provenance. *Island Arc*, **27**, e12258. doi:10.1111/iar.12258.

Matsuoka, A. (1987) Radiolarian age of the Shiriya Group in Aomori Prefecture, northeast Japan. *Fossils*, **42**, 7–13 (in Japanese with English abstract).

Matsuoka, A. (1995) Jurassic and Lower Cretaceous radiolarian zonation in Japan and in the western Pacific. *The Island Arc*, **4**, 140–153.

Matsuoka, A. and Oji, T. (1990) Middle Jurassic radiolarian fossils from the Magisawa Formation in the Taro Belt, North Kitakami Mountains. *The Journal of the Geological Society of Japan*, **96**, 239–241 (in Japanese).

Minoura, K. (1985) Where did the Kitakami and Abukuma Massif come from?: How to develop the geological structure of the Tohoku of Japan. *Kagaku*, **55**, 14–23 (in Japanese).

Minoura, K. and Tsushima, H. (1984) Geology of the Omoto district in the eastern margin of the North Kitakami Massif. *The Science Report of the Hirosaki University*, no. 31, 93–107 (in Japanese).

Murata, M. (1962) The Upper Jurassic of Cape Shiriya, Aomori Prefecture, Japan. *The Science Reports of the Tohoku University, Series 2, Special Volume*, no. 5, 119–126.

Murata, M. and Nagai, T. (1972) Discovery of conodonts from Sekkenai, Hiranai-cho, Higashi-Tsugaru-gun, Aomori Prefecture, Japan. *Professor Jun-ichi Iwai Memorial Volume*, 709–717.

Murata, M., Nagai, T. and Kawamura, S. (1974) Signification and occurrence of late Carboniferous conodont fossil from Cape Kodomari, Tsugaru Peninsula, Aomori Prefecture, Japan. *Aomori-Chigaku*, no. 26, 3–5 (in Japanese). http://aomorichigaku.web.fc2.com/fc2-imageviewer/?aid=1&iid=24 (Accessed:2019-02-14)

Nakae, S. and Kamada, K. (2003) Late Jurassic radiolarians from the Rikuchu-Seki district in the North Kitakami Belt, Northeast Japan. *The Journal of the Geological Society of Japan*, **109**, 722–725 (in Japanese with English abstract).

Nakae, S. and Kurihara, T. (2011) Direct age determination for an Upper Permian accretionary complex (Kirinai Formation), Kitakami Mountains, Northeast Japan. *Palaeoworld*, **20**, 146–157.

Nishizono, Y. (1996) Mesozoic convergent process of the Southern Chichibu Terrane in west Kyushu, Japan, on the basis of Triassic to Early Cretaceous radiolarian biostratigraphy. *Kumamoto Journal of Science, Earth Sciences*, **14**, 45–226.

O'Dogherty, L., Bill, M., Goričan, S., Dumitrica, P. and Masson, H. (2006) Bathonian radiolarians from an ophiolitic mélange of the Alpine Tethys (Gets Nappe, Swiss–French Alps). *Micropaleontology*, **51**, 425–485.

O'Dogherty, L., Goričan, Š. and Gawlick, H.-J. (2017) Middle and Late Jurassic radiolarians from the Neotethys suture in the Eastern Alps. *Journal of Paleontology*, **91**, 25–72.

Oho, Y. and Iwamatsu, A. (1986) Olistostrome in the Shiriyazaki area of the Shimokita Peninsula, Northeast Japan. *The Journal of the Geological Society of Japan*, **92**, 109–118 (in Japanese with English abstract).

Onuki, Y. (1959) Discovery of Hexacorals from the Shiriya district, Aomori Prefecture, Northeast Japan. *The Journal of the Geological Society of Japan*, **65**, 248 (in Japanese).

Otoh, S. and Sasaki, M. (2003) Tectonostratigraphic division and regional correlation of the sedimentary complex of the North Kitakami Belt. *Journal of Geography (Chigaku Zasshi)*, **112**, 406–410.

Ožvoldová, L., Jablonsky, J. and Frantova, L. (2000) Upper Jurassic radiolarites of the Czertezic succession and comparison with the Kysuca succession in the east-Slovak part of the Pienny Klippen Belt (western Carpathians, Slovakia). *Geologica Carpathica*, **51**, 109–119.

Sano, S., Sugisawa, N. and Shimaguchi, T. (2009) Discovery of megalodontoid bivalves in the Shiriya area, northern Honshu, Northeast Japan, and its geological implications. *Memoir of the Fukui Prefectural Dinosaur Museum*, **8**, 51–57 (in Japanese with English abstract).

Sagong, H., Kwon, S.-T. Ree, J.-H. (2005) Mesozoic episodic magmatism in South Korea and its tectonic implication. *Tectonics*, **24**, TC5002, doi:10.1029/2004TC001720.

Steiger, T. (1992) Systematik, stratigraphie und Palökologie der Radiolarien des Oberjura-Unterkrieden-Grenzbereiches im Osterhorn-Tirolikum (Nördliche Kalkalpen, Salzburg und Bayern). *Zitteliana*, **19**, 3–188.

Suzuki, N. and Ogane, K. (2004) Paleoceanographic affinities of radiolarian faunas in late Aalenian time (Middle Jurassic) recorded in the Jurassic accretionary complex of Japan. *Journal of Asian Earth Sciences*, **23**, 343–357.

Suzuki, N., Ehiro, M., Yoshihara, K., Kimura, Y., Kawashima, G., Yoshimoto, H. and Nogi, T. (2007a) Geology of the Kuzumaki–Kamaishi Subbelt of the North Kitakami Belt (a Jurassic accretionary complex), Northeast Japan: Case study of the Kawai–Yamada area, eastern Iwate Prefecture. *Bulletin of the Tohoku University Museum*, no. 6, 103–174.

Suzuki, N., Yamakita, S., Takahashi, S. and Ehiro, M. (2007b) Middle Jurassic radiolarians from carbonate manganese nodules in the Otori Formation in the eastern part of the Kuzumaki–Kamaishi Subbelt, the North Kitakami Belt, Northeast Japan. *The Journal of the Geological Society of Japan*, **113**, 274–277 (in Japanese with English abstract).

Toyohara, F., Uesugi, K., Kimura, T., Ito, T., Murata, A. and Iwamatsu, A. (1980) Northern Kitakami Massif: Geosynclines in the Oshima Peninsula. *In* Kimura, T., ed., *Reexamination of geosynclines and tectonic division on the northern part of the Japanese Islands*, Science Report (Fund type A) for Grants-in-Aid for Scientific Research (The Ministry of Education, Science, Sports and Culture), Tokyo University, 27–36 (in Japanese).

Tsushima, K. and Takizawa, F. (1977) *Geology of the Shiriyazaki District. With Geological Sheet Map at 1:50,000*, Geological Survey of Japan. 36p (in Japanese with English abstract).

Uchino, T. (2017) Late Triassic U–Pb-zircon age from tuffaceous mudstone in the Kadoma Complex, North Kitakami Belt, Northeast Japan. *The Journal of the Geological Society of Japan*, **123**, 977–982 (in Japanese with English abstract).

Uchino, T. (2018a) Detrital zircon U–Pb age of the Jurassic accretionary complex in the western area of Lake Towada located between Akita and Aomori prefectures, Northeast Japan. *Bulletin of Geological Survey of Japan*, **69**, 37–46 (in Japanese with English abstract).

Uchino, T. (2018b) Detrital zircon U–Pb age of sandstone within the Jurassic accretionary complex in the Omori area, northeastern Shimokita Peninsula, Northeast Japan. *Bulletin of Geological Survey of Japan*, **69**, 125–133 (in Japanese with English abstract).

Uchino, T. (2019) Detrital zircon U–Pb ages of sandstone within the Jurassic accretionary complex in the North Kitakami Belt of the Sotoyama District, Iwate Prefecture, Northeast Japan. *Bulletin of Geological Survey of Japan*, **70**, 357–372 (in Japanese with English abstract).

Ueda, H., Mori, M. and Sato, I. (2009) Early Jurassic radiolarian fossils from mudstone within an accretionary complex south of Hirosaki City, Aomori Prefecture, Japan. *The Journal of the Geological Society of Japan*, **115**, 610–613 (in Japanese with English abstract).

Ueda, H., Kimura, S., Saito, T., Takano, Y., Iizuka, N. and Orihashi, Y. (2018) Material recycling in a sediment-starved trench recorded in the Early Cretaceous Shiriya accretionary complex, Northeast Japan. *Island Arc*, **27**, e12272. doi:10.1111/iar.12272.

Yang, Q. and Matsuoka, A. (1997) A comparative study on Upper Jurassic radiolarian biostratigraphy of the Taman Formation, east-central Mexico and the ODP Site 801B Section, west Pacific. *Science Reports of Niigata University, Series E (Geology)*, no. 12, 29–49.

Yoshihara, K., Suzuki, N. and Ehiro, M. (2002) Middle Jurassic radiolarian-bearing nodules from the Kuzumaki-Kamaishi Subbelt in the northern Kitakami Massif and its significance. *The Journal of the Geological Society of Japan*, **108**, 536–539 (in Japanese with English abstract).

Zügel, P., Riegraf, W., Schweigert, G. and Dietl, G. (1998) Radiolaria from the Nusplingen Lithographic Limestone (Late Kimmeridgian, SW Germany). *Stuttgarter Beiträge zur Naturkunde, Serie B*, no. 268, 1–44.

Recieved July 9, 2019
Accepted March 12, 2020
Published on-line May 7, 2020

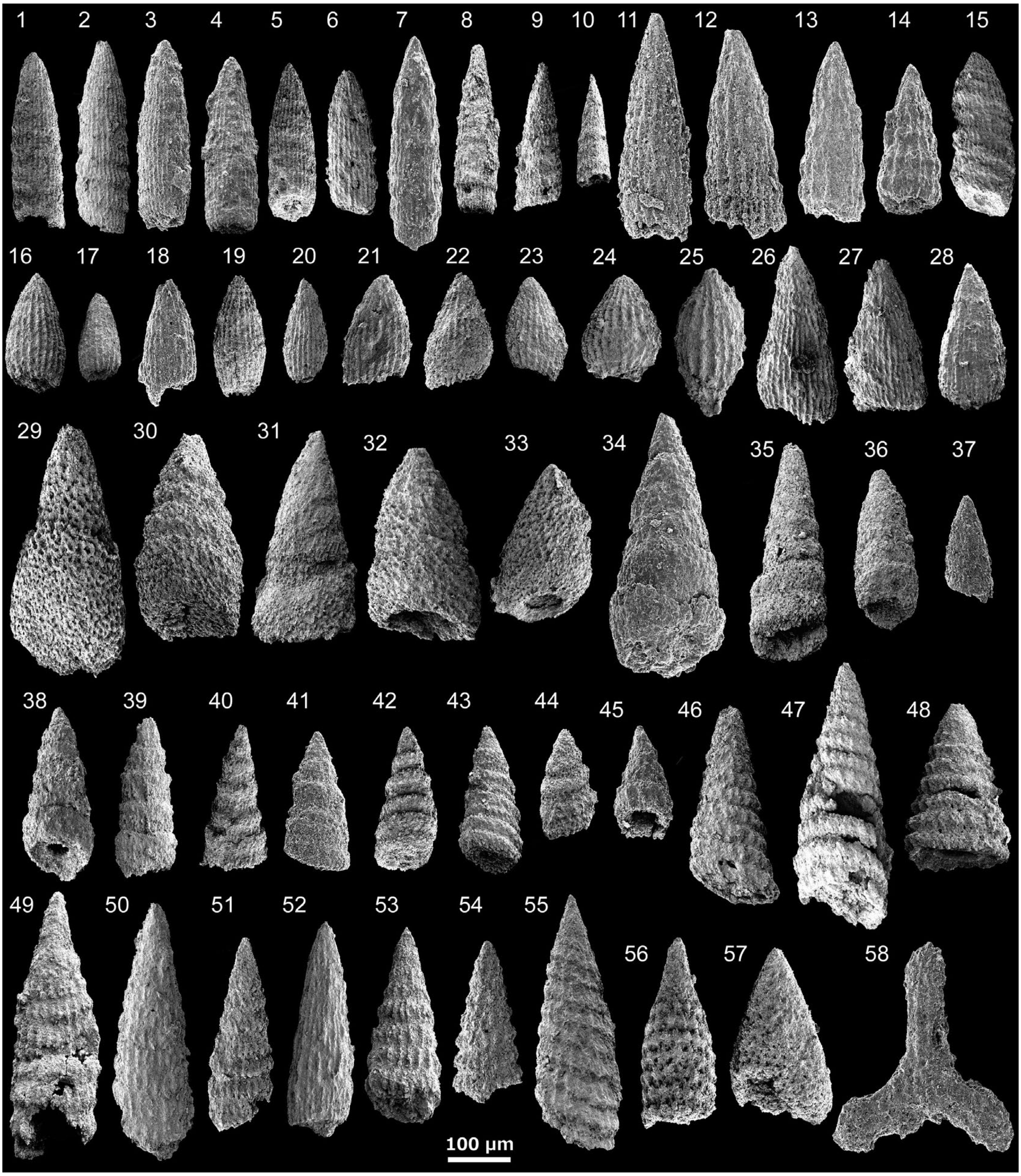

Plate 1 Scanning electron microscopy images of the Kimmeridgian (middle Late Jurassic) radiolarians extracted from mudstone at Loc. 1. **1**–**3**: *Archaeodictyomitra spelae* Chiari, Cortese and Marcucci, **4**–**6**: *Archaeodictyomitra* cf. *spelae* Chiari, Cortese and Marcucci, **7**: *Archaeodictyomitra* aff. *prisca* Kozur and Mostler, **8**: *Archaeodictyomitra* sp. A, **9**–**10**: *Archaeodictyomitra* sp. B, **11**–**14**: *Archaeodictyomitra* aff. *vulgaris* Pessagno, **15**: *Archaeodictyomitra* cf. *unica* Wu, **16**–**17**: *Archaeodictyomitra* aff. *rigida* Pessagno, **18**–**20**: *Archaeodictyomitra* aff. *suzukii* Aita, **21**–**23**: *Archaeodictyomitra* cf. *inornata* Hull, **24**: *Archaeodictyomitra* sp. C, **25**: *Archaeodictyomitra* sp. D, **26**–**28**: *Parahsuum mudongensis* (Li) sensu lato, **29**–**31**: *Spongocapsula palmerae* Pessagno, **32**–**33**: *Spongocapsula* sp., **34**–**36**: *Spongocapsula*? sp., **37**: *Loopus* cf. *venusta* (Chiari, Cortese and Marucci), **38**–**43**: *Cinguloturris* cf. *carpatica* Dumitrică, **44**: *Cinguloturris* cf. *latiannulatum* (Grill and Kozur), **45**: *Cinguloturris* sp., **46**–**47**: *Svinitzium* sp., **48**: *Wrangellium* sp., **49**–**55**: *Transhsuum* sp., **56**–**57**: Nassellaria gen. et sp. indet., **58**: Pyloniodea et sp. indet.

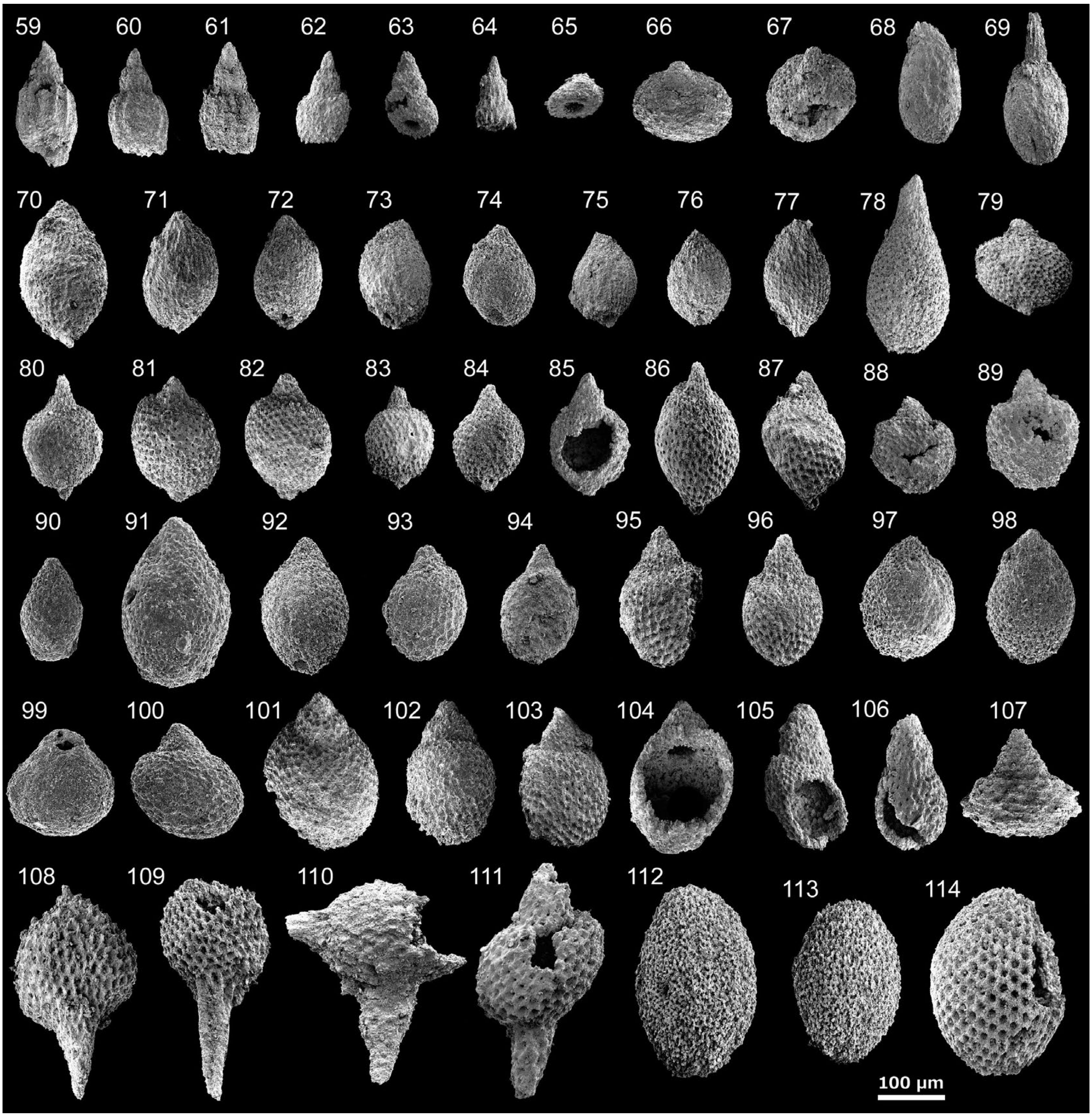

Plate 1 (Continued)

59–**61**: *Eucyrtidiellum* cf. *pyramis* (Aita), **62**: *Eucyrtidiellum* cf. *nodosum* Wakita, **63**: *Crococapsa* aff. *truncata* (Wu), **64**–**68**: Nassellaria gen. et sp. indet., **69**: *Kilinora* sp., **70**: *Striatojaponocapsa* cf. *conexa* (Matsuoka), **71**–**76**: *Striatojaponocapsa synconexa* O'Dogherty, Goričan and Dumitrică, **77**: *Striatojaponocapsa* sp., **78**: *Praewilliriedellum* sp., **79**: *Hemicryptocapsa carpathica* (Dumitrică), **80**–**87**: *Williriedellum* sp., **88**–**89**: *Minutosolla* sp., **90**: *Praezhamoidellum*? sp., **91**–**92**: *Hiscocapsa robusta* (Matsuoka), **93**: *Hemicryptocapsa* cf. *yaoi* (Kozur), **94**–**98**: *Praezhamoidellum* sp., **99**: *Zhamoidellum* sp., **100**: *Zhamoidellum* cf. *ventricosum* Dumitrică, **101**–**104**: *Zhamoidellum ovum* Dumitrică, **105**–**106**: *Complexapora* aff. *kiesslingi* Hull, **107**: Minocapsidae gen. et sp. indet., **108**: *Archaeospongoprunum* sp., **109**: *Archaeospongoprunum* cf. *mizutanii* Ožvoldová, **110**: *Podobursa* sp., **111**: *Favosyringium* cf. *affine* (Rüst) sensu Steiger (1992), **112**–**113**: *Bistarkum* aff. *mangartense* Goričan, Šmuc and Baumgartner, **114**: Nassellaria gen. et sp. indet.

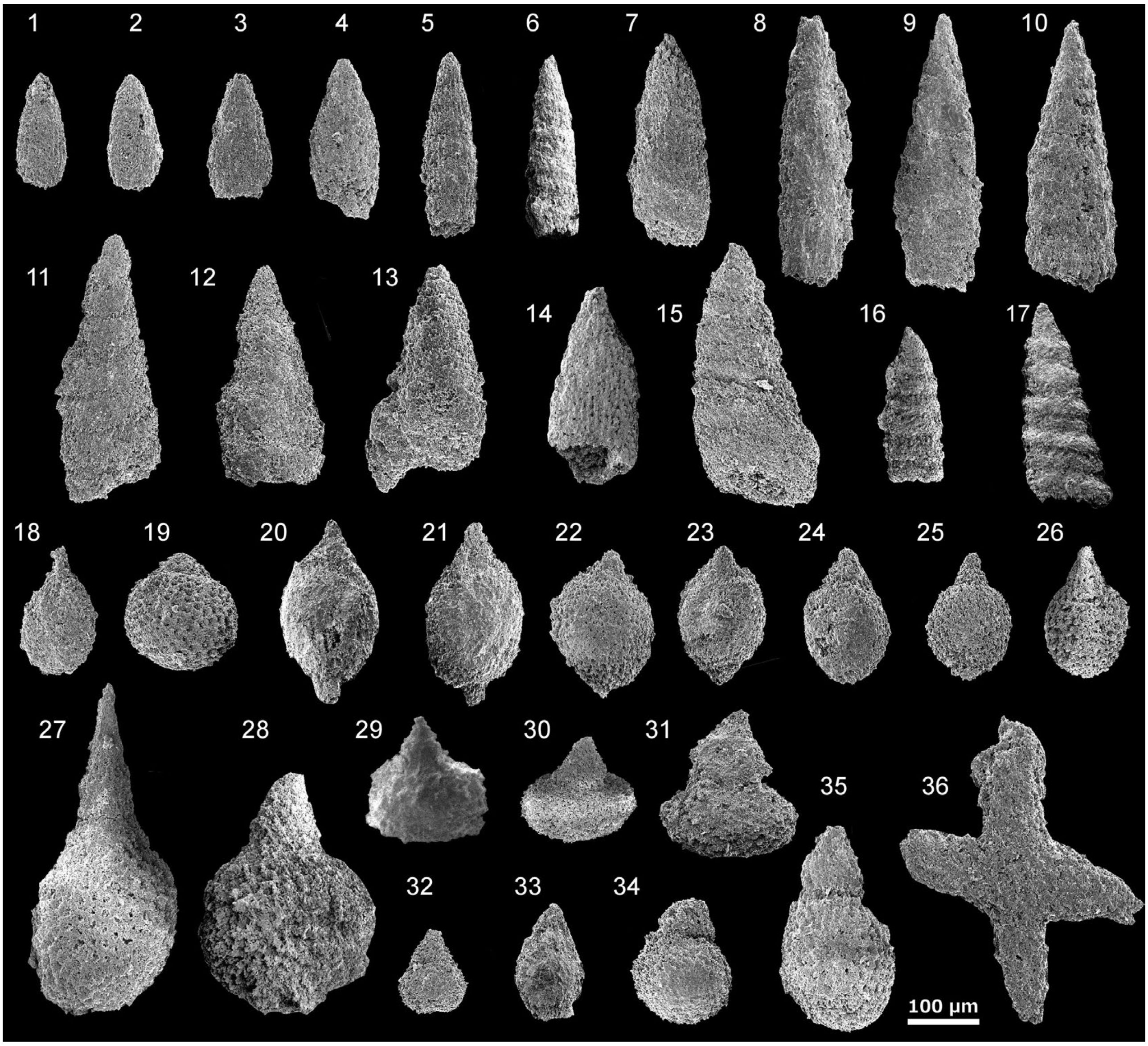

Plate 2 Scanning electron microscopy images of probably Callovian–Kimmeridgian radiolarians extracted from mudstone at Loc. 2. **1–2**: *Archaeodictyomitra* aff. *rigida* Pessagno, **3**: *Archaeodictyomitra* cf. *tyaughtonensis* Cordey, **4**: *Archaeodictyomitra* cf. *inornata* Hull, **5–14**: Multisegmented nassellarians, **15**: *Cinguloturris* cf. *floridicingula* (Li), **16**: *Cinguloturris* cf. *getsensis* O'Dogherty, Goričan and Dumitrică, **17**: *Cinguloturris* cf. *carpatica* Dumitrică, **18**: Spherical radiolarians, **19**: *Zhamoidellum* cf. *mikamense* Aita, **20–23**: *Williriedellum* sp., **24–26**: Williriedelloidea gen. et sp. indet., **27–28**: Syringocapsidae? gen. et sp. indet., **29**: *Eucyrtidiellum* sp., **30**: *Quarkus* sp., **31**: *Tetracapsa* sp., **32–35**: Few segmented nassellarians, **36**: Four-armed flat Pylonioidea.

下北半島北東部，北部北上帯の U–Pb 年代測定砂岩近傍の泥岩から得られた後期ジュラ紀放散虫化石

内野　隆之・鈴木　紀毅

要　旨

青森県下北半島の北東部では，北部北上帯に属する付加体が，桑畑山（くわばたやま）地域，片崎山地域，大森地域に分布している．桑畑山地域の付加体については，後期ジュラ紀の岩屋ユニットと前期白亜紀前半の尻労（しつかり）ユニットに区分されるなど，これまで多くの研究がなされているものの，片崎山・大森地域の付加体については，大森地域の砂岩から砕屑性ジルコン U–Pb 年代が得られているほかは，詳しいデータはほとんどない．

本研究ではジルコン年代が測定された砂岩近傍の泥岩から *Eucyrtidiellum* cf. *pyramis* をはじめとする後期ジュラ紀（おそらくキンメリッジアン期）の放散虫化石が見出された．この泥岩の化石年代と砂岩のジルコン年代とは大差なく，また泥岩と砂岩との層準の間に不連続構造面も確認されないことから，両者の堆積年代に大きな乖離はないと考えられる．

岩相・地質構造・放散虫化石年代から，片崎山・大森地域の付加体と，桑畑山地域の岩屋ユニットは対比可能である．つまり，下北半島北東部の付加体は，後期ジュラ紀に形成された桑畑山地域の岩屋ユニット及び片崎山・大森地域の未命名ユニットと，前期白亜紀に形成された桑畑山地域の尻労ユニットとに区分される．

難読･重要地名

Chikagawa：近川，Higashidori：東通，Iwaya：岩屋，Kadoma：門馬，Katasakiyama；Mt. Katasaki：片崎山，Kuwabatayama；Kuwabatakeyama；Mt. Kuwabata：桑畑山，Mt. Noborimori：登森，Mt. Omori；Omori：大森，Mt. Toyamori：トヤ森，Magisawa：槇木沢，Magidai：間木平，Sarugamori：猿ヶ森，Shimokita：下北，Shiriya：尻屋，Shiriyazaki：尻屋崎，Shitsukari：尻労，Takayashiki：高屋敷，Tatemachijima：立待島